Journal of Sound and Vibration 330 (2011) 4676–4688

Contents lists available at ScienceDirect

Journal of Sound and Vibration

journal homepage: www.elsevier.com/locate/jsvi

Stabilization of an axially moving web via regulation of axial velocity

Quoc Chi Nguyen [a,1], Keum-Shik Hong [b,*]

[a] School of Mechanical Engineering, Pusan National University, San 30 Jangjeon-dong, Geumjeong-gu, Busan 609-735, Republic of Korea
[b] Department of Cogno-Mechatronics Engineering and School of Mechanical Engineering, Pusan National University, San 30 Jangjeon-dong, Geumjeong-gu, Busan 609-735, Republic of Korea

ARTICLE INFO

Article history:
Received 17 September 2010
Received in revised form
20 April 2011
Accepted 21 April 2011
Handling Editor: J. Lam
Available online 10 May 2011

ABSTRACT

In this paper, a novel control algorithm for suppression of the transverse vibration of an axially moving web system is presented. The principle of the proposed control algorithm is the regulation of the axial transport velocity of an axially moving beam so as to track a profile according to which the vibration energy decays most quickly. The optimal control problem that generates the proposed profile of the axial transport velocity is solved by the conjugate gradient method. The Galerkin method is applied in order to reduce the partial differential equation describing the dynamics of the axially moving beam into a set of ordinary differential equations (ODEs). For control design purposes, these ODEs are rewritten into state-space equations. The vibration energy of the axially moving beam is represented by the quadratic form of the state variables. In the optimal control problem, the cost function modified from the vibration energy function is subjected to the *constraints* on the state variables, and the axial transport velocity is considered as a control input. Numerical simulations are performed to confirm the effectiveness of the proposed control algorithm.

1. Introduction

There are numerous industries that use web-material transport systems such as papers, textiles, metals, polymers, and composites. In these systems, the application of roll-to-roll processing yields better performance and supports mass production and high-speed automation. However, the mechanical vibrations (particularly in the transverse direction) of web materials have been the main quality- and productivity-limiting factor, especially in high-speed roll-to-roll systems. The present work was motivated by the vibration control problem in roll-to-roll lithography systems, and indeed, it should be noted that the lithographic process is a key manufacturing technology in flexible electronics. For example, Fig. 1 depicts the roll-to-roll patterning system of the Anvik Corporation [1]. In this system, the flexible substrate web, which is fed from a supply roll, extends across the exposure region on the scanning stage, and is wound onto a take-up roll. When the moving web comes to a stop, residual transverse vibrations arise naturally, even if the transport velocity of the moving web approaches the zero value. Therefore, the lithographic process has to be suspended until the web reaches a tolerable, minimal vibration state. In spite of the fact that the moving web, which can be considered as an axially moving viscoelastic beam, can be stabilized by the viscous damping force if the axial transport velocity is less than the critical value [2], this usually requires plenty of time. This process suspension due to the vibrations of moving materials is a typical technical problem in almost all roll-to-roll systems. Therefore, reasonably prompt vibration suppression of moving materials for improvement of the control performance of high-speed roll-to-roll systems is desirable.

* Corresponding author. Tel.: +82 51 510 2454; fax: +82 51 514 0685.
E-mail addresses: nqchi@pusan.ac.kr (Q.C. Nguyen), kshong@pusan.ac.kr (K.-S. Hong).
[1] Tel.: +82 51 510 1481; fax: +82 51 514 0685.

0022-460X/$ - see front matter
doi:10.1016/j.jsv.2011.04.029

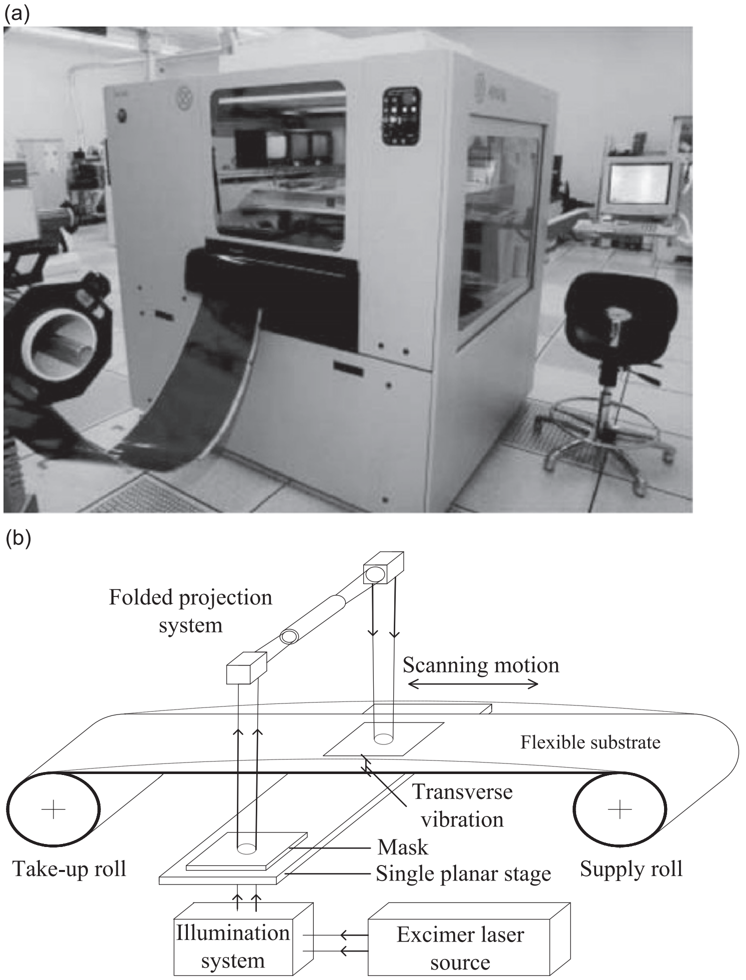

Fig. 1. Example of large-area high-throughput roll-to-roll patterning system [1]: (a) picture (© [2005] IEEE) and (b) schematic.

Vibration control schemes for axially moving strings include Refs. [3–13]. Those for axially moving beams include Refs. [14–19]. Boundary control techniques for axially moving systems have been developed in Refs. [4–19]. These achievements were predicated on the Lyapunov energy-based method. They show that boundary control is an efficiency control technique to stabilize axially moving systems. However, referring again to the practical example of the lithography roll-to-roll system, control forces exerted from boundary actuators might destroy the surface of the substrate material. Therefore, boundary control is not a suitable solution for vibration control in flexible electronics. The distributed control method [3], which uses pneumatic diffusers to generate the distributed control forces, is a possibility, but the disadvantage is that implementation of the control algorithm requires distributed feedback signals. It should be noted that setting up a distributed sensor system for an axially moving system is not feasible in practice. Therefore, developing a proper control method to suppress the transverse vibrations of moving webs in flexible electronics as well as axially moving systems, where application of boundary control, at least thus far, is impossible, represents a formidable challenge. This paper presents, as a means of overcoming that difficulty, a novel control algorithm that employs the effects of the time-varying axial transport velocity of the moving web to suppress transverse vibration. This control algorithm not only solves the technical difficulty but also, because it requires no actuator, provides cost-effectiveness.

In investigations of the dynamics of translating as well as stationary continua, a number of approximate methods have been used [2,20–36]. For instance, in the case of time-dependent axial velocity, approximate solutions were obtained in Ref. [23] with the method of multiple time scales, whereas in Ref. [32], the Laplace transform method was employed. A state space form of equations of motion for an axially moving magnetic tape was obtained using the skew-symmetric differential operator in Ref. [33], and the transverse vibration of the axially moving magnetic tape was approximated by the eigenfunction expansion. In Refs. [2,24–31,34–36] the transverse displacement of an axially moving beam was expanded into a Fourier series (a sine series is a good candidate), and the Galerkin method was applied to reduce the partial differential equation (PDE), which governs transverse motion, into a set of ordinary differential equations (ODEs), a dimensional discrete model. The discrete models obtained using the Galerkin method were compared with results presented in the literature, and good agreements were shown in Refs. [24,26,27,31,34]. In Ref. [29], experimental results were consistent with numerical simulation results of dynamic responses of an axially moving belt using a high dimensional discrete model. Indeed, the aforementioned studies have shown that the Galerkin method gives good predictions of the dynamic responses of axially moving systems.

In this paper, a novel control algorithm for suppression of the transverse vibration of an axially moving web is presented. Contrary to the conventional methods (boundary and distributed controls) that use external forces to stabilize axially moving systems, the proposed control algorithm is implemented by the regulation of the axial transport velocity, which is a system parameter. The remainder of this paper is organized as follows. Section 2 introduces a dynamic model of the considered system (an axially moving viscoelastic beam) approximated by means of the Galerkin method. Subsequently, the approximate dynamic model is rewritten into state-space equations. Section 3 presents our control algorithm, which utilizes the effects of the time-varying axial transport velocity to suppress the transverse vibration. The idea is to regulate the axial transport velocity of the axially moving beam to track a profile, according to which the vibration energy decreases most quickly. Section 4 illustrates the effectiveness of the proposed control algorithm with numerical simulations. Finally, Section 5 draws conclusions.

2. Problem formulation

In practice, besides the transverse motion of the axially moving web, the lateral motion of the web caused from the misalignment of the rolls may occur. However, the lateral motion can be eliminated if the misalignment of the rolls is significantly reduced by precision manufacturing, and the axes of rotation of the rolls are well controlled by terminal web guide mechanisms. Therefore, only the transverse motion (transverse vibration) of the moving web is considered in this paper. Based on this assumption, the axially moving web is modeled as an axially moving viscoelastic beam [15,27,33]. Fig. 2 shows the axially moving beam traveling between two fixed rolls, considered as the left and right boundaries. These boundaries are fixed in the sense that vertical movement of the beam is restricted. Let t be the time and x be the spatial coordinate along the longitude of motion. The equation of motion of the axially moving beam is given as [15,21,28,31,33]

$$a^2 w_{xxxx}(x,t) - (c^2 - v^2(t)) w_{xx}(x,t) + 2v(t) w_{xt}(x,t) + w_{tt}(x,t) + b w_t(x,t) + (bv(t) + \dot{v}(t)) w_x(x,t) = 0, \tag{1}$$

where $a = \sqrt{EI/\rho A}$, $b = d_v/\rho A$, and $c = \sqrt{P/\rho A}$. In Eq. (1), the variable $w(x,t)$ denotes the transverse displacement at the spatial coordinate x and time t; l is the distance between two fixed rolls; ρ is the mass per unit length of the beam; d_v is the viscous damping coefficient; and $v(t)$ is the time-varying axial velocity of the beam. Moreover, let A be the cross-section of the beam, E is the Young's modulus, I is the moment of inertia of the beam's cross-section about the z-axis, and P is the axial tension. The beam model is obtained under the assumption that the tension P and the mass per unit length ρ are constants. The beam system is considered with the simple boundary conditions:

$$w(0,t) = 0, \quad w(l,t) = 0, \tag{2}$$

$$w_{xx}(0,t) = 0, \quad w_{xx}(l,t) = 0, \tag{3}$$

It should be noted that the established boundary conditions are consistent with the practical example of the roll-to-roll lithography system presented in Section 1, where the transverse vibration resulting from eccentricity between two fixed rolls is ignored. The initial transverse displacement and the initial transverse velocity are given as, respectively,

$$w(x,0) = w_0(x) \quad \text{and} \quad w_t(x,0) = w_{t0}(x). \tag{4}$$

To obtain a finite-dimensional dynamic model, the Galerkin method is applied to solve the PDE (1). The transverse displacement $w(x,t)$ is assumed to be expanded as

$$w(x,t) = \sum_{i=1}^{n} q_i(t) \varphi(x), \tag{5}$$

where $\varphi(x) = \sin(i\pi x/l)$ describes the effect of the ith eigenvalue of the stationary beam, and $q_i(t)$ represents the generalized transverse displacement [31]. The finite-dimensional dynamic system will be obtained by carrying out the following procedure: (i) multiplying Eq. (1) by a weighting function $\varphi(x)$, (ii) integrating the resultant equation obtained in

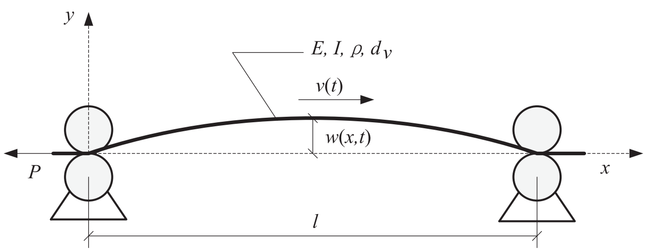

Fig. 2. Axially moving beam traveling between two fixed rolls.

step (i) over the domain $x \in [0,l]$, (iii) utilizing the boundary conditions (2) and (3) and substituting Eq. (5) into the resultant equation obtained in step (ii), and (iv) collecting all terms of the resultant equation obtained in step (iii) with respect to $q_i(t)$, $\dot{q}_i(t)$, and $\ddot{q}_i(t)$. The equations obtained in steps (i)–(iii) are similar to the results found in Refs. [2, p. 182] and [31, p. 320]. After step (iv), the PDE (1) can be rewritten into a set of ODEs [2,24–31,34–36] as

$$M\ddot{\mathbf{q}}(t)+\mathbf{C}(t)\dot{\mathbf{q}}(t)+\mathbf{K}(t)\mathbf{q}(t)=0, \tag{6}$$

where the elements of the mass matrix $\mathbf{M}$, the damping matrix $\mathbf{C}(t)$, and the stiffness matrix $\mathbf{K}(t)$ are defined as

$$M_{ji}=\int_0^l \sin(i\pi x/l)\sin(j\pi x/l)\mathrm{d}x=\begin{cases} l/2, & \text{if } i=j, \\ 0, & \text{if } i\neq j, \end{cases} \tag{7}$$

$$C_{ji}=(2i\pi v(t)/l)\int_0^l \cos(i\pi x/l)\sin(j\pi x/l)\mathrm{d}x+b\int_0^l \sin(i\pi x/l)\sin(j\pi x/l)\mathrm{d}x,$$

$$C_{ji}=\begin{cases} bl/2, & \text{if } i=j, \\ 0, & \text{if } i\neq j,\ i+j \text{ is even}, \\ 4ijv(t)/(j^2-i^2), & \text{if } i\neq j,\ i+j \text{ is odd}, \end{cases} \tag{8}$$

$$K_{ji}=a^2(i\pi/l)^4\int_0^l \sin(i\pi x/l)\sin(j\pi x/l)\mathrm{d}x+(i\pi/l)^2(c^2-v^2(t))\int_0^l \sin(i\pi x/l)\sin(j\pi x/l)\mathrm{d}x$$
$$+(i\pi(bv(t)+\dot{v}(t))/l)\int_0^l \cos(i\pi x/l)\sin(j\pi x/l)\mathrm{d}x,$$

$$K_{ji}=\begin{cases} a^2(i\pi/l)^4+(i\pi/l)^2(c^2-v^2(t)), & \text{if } i=j, \\ 0, & \text{if } i\neq j,\ i+j \text{ is even}, \\ 2ij(bv(t)+\dot{v}(t))/(j^2-i^2), & \text{if } i\neq j,\ i+j \text{ is odd}. \end{cases} \tag{9}$$

Therefore, it is convenient to rewrite the ODEs (6) in the state space [26] as

$$\dot{\mathbf{s}}(t)=\mathbf{A}(t)\,\mathbf{s}(t), \tag{10}$$

where

$$\mathbf{s}(t)=(\dot{\mathbf{q}}^{\mathrm{T}}(t),\ \mathbf{q}^{\mathrm{T}}(t))^{\mathrm{T}}, \tag{11}$$

and

$$\mathbf{A}(t)=\begin{bmatrix} -\mathbf{M}^{-1}\mathbf{C}(t) & -\mathbf{M}^{-1}\mathbf{K}(t) \\ \mathbf{I}_{n\times n} & \mathbf{0}_{n\times n} \end{bmatrix}. \tag{12}$$

Remark 1. The number of functions n in the approximate solution (5) affects to the convergence of the sine series as well as the smoothness of the function $w(x,t)$. The method for choosing n can be found in Ref. [29, Section 3].

Remark 2. For control design purposes, the linear operator $\mathbf{A}$ combined with the approximate solution (5) will be used to describe the dynamics of the axially moving beam system. It is obvious that the matrices $\mathbf{C}(t)$ and $\mathbf{K}(t)$, and consequently $\mathbf{A}(t)$, are functions of the axial transport velocity $v(t)$. This allows the eigenvalues of the linear operator $\mathbf{A}$ as well as the convergence speed, when $\mathbf{s}(t)\to 0$, to be adjusted by changing the axial transport velocity. On this technical basis, a control algorithm that utilizes the effects of the axial transport velocity to suppress the transverse vibration was developed.

3. Control design

Fig. 3 illustrates the idea of the proposed control algorithm. In the case of no control for vibration suppression, the axial transport velocity is regulated to decrease from $v(0)$ to zero using a conventional profile constructed from a slope; that is, the transport deceleration is constant. The conventional constant-deceleration profile shown in Fig. 3(a) is a typical example widely used in practice. In this case, the vibration energy $E_{\mathrm{beam}}(t)$ tends naturally to zero in the presence of the viscous damping. However, the phenomenon that the residual vibration energy still has considerable value when the axial transport velocity arrives at zero usually occurs. Moreover, the convergence of the vibration energy to zero depends on the value of the viscous damping coefficient of the web material. It should be noted that the viscous damping coefficients of the web materials (for example: films, textiles, and plastics) may not be large enough to dissipate significant vibration energy. Therefore, vibration suppression that relies only on the viscous damping force usually requires plenty of time. As shown in Fig. 3(b), when the control algorithm is applied, the axial transport velocity is regulated to track a profile constructed from several slopes instead of the conventional constant-deceleration profile. This control algorithm is expected to impart two improvements to control performance. First, the vibration energy is expected to decay quickly.

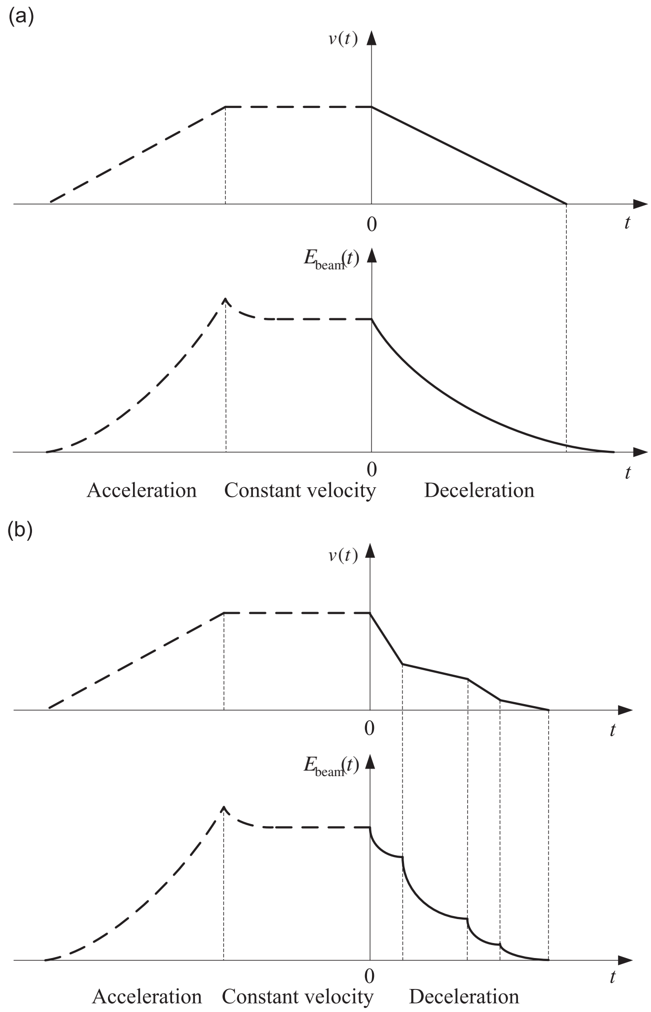

Fig. 3. Comparison of the axial velocities and the transverse vibration energies (only deceleration period is focused): (a) with the proposed velocity profile and (b) with the conventional velocity profile.

Second, when the axial transport velocity reaches the zero value, the transverse vibration is suppressed completely. These improvements were validated both by theoretical calculations (see Eqs. (29)–(42)) and numerical simulation results. To obtain the proposed profile, a control optimal problem was established, in which the cost function is modified from the vibration energy function of the beam system, and the time-varying axial transport velocity is considered as a control input. The conjugate gradient (CG) method [37–44] was used to solve the optimal control problem. The application of the CG method provides a good convergence property for the cost function as well as the vibration energy. As shown in Fig. 4, the vibration energy of the moving web tends to the minimum point (the zero value) in a zigzag fashion; that is, in every iteration of the CG algorithm, the axial transport velocity is regulated so that the vibration energy function $E_{\text{beam}}(t)$ decreases in the direction opposite to the gradient of the vibration energy, where $E_{\text{beam}}(t)$ decreases most quickly.

The state-space model (10) is rewritten as

$$\dot{\mathbf{s}}(t) = \mathbf{f}(\mathbf{s}, v, \dot{v}) = \mathbf{A}_c\mathbf{s}(t) + v(t)\mathbf{B}_1\mathbf{s}(t) + v^2(t)\mathbf{B}_2\mathbf{s}(t) + (bv(t) + \dot{v}(t))\mathbf{B}_3\mathbf{s}(t), \tag{13}$$

where $\mathbf{A}_c$ and $\mathbf{B}_i (i=1,\ 2,\ 3)$ are constant matrices. The elements of $\mathbf{A}_c$ and $\mathbf{B}_i (i=1,\ 2,\ 3)$ are defined as

$$\mathbf{A}_c = \begin{bmatrix} -\mathbf{M}^{-1}\mathbf{C}^s & -\mathbf{M}^{-1}\mathbf{K}^s \\ \mathbf{I}_{n\times n} & \mathbf{0}_{n\times n} \end{bmatrix}, \tag{14}$$

where

$$C_{ji}^s = \begin{cases} bl/2, & \text{if } i=j, \\ 0, & \text{if } i \neq j, \end{cases} \tag{15}$$

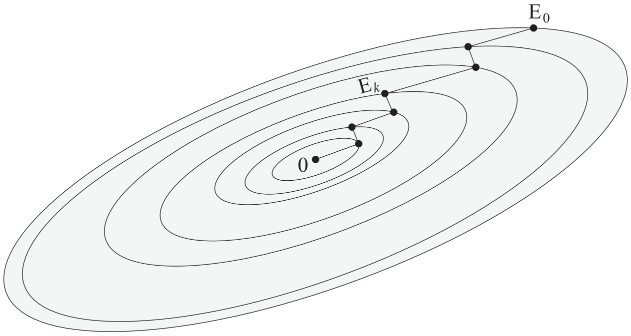

Fig. 4. Convergence of the vibration energy in zigzag fashion.

$$K^s_{ji} = \begin{cases} a^2(i\pi/l)^4+(i\pi/l)^2c^2, & \text{if } i=j, \\ 0, & \text{if } i\neq j. \end{cases} \tag{16}$$

$$\mathbf{B}_1 = \begin{bmatrix} -\mathbf{M}^{-1}\mathbf{B}^s_1 & \mathbf{0}_{n\times n} \\ \mathbf{0}_{n\times n} & \mathbf{0}_{n\times n} \end{bmatrix}, \tag{17}$$

where

$$B^s_{1ji} = \begin{cases} 0, & \text{if } i=j, \\ 0, & \text{if } i\neq j,\ i+j \text{ is even}, \\ 4ij/(j^2-i^2), & \text{if } i\neq j,\ i+j \text{ is odd}. \end{cases} \tag{18}$$

$$\mathbf{B}_2 = \begin{bmatrix} \mathbf{0}_{n\times n} & -\mathbf{M}^{-1}\mathbf{B}^s_2 \\ \mathbf{0}_{n\times n} & \mathbf{0}_{n\times n} \end{bmatrix}, \tag{19}$$

where

$$B^s_{2ji} = \begin{cases} -(i\pi/l)^2, & \text{if } i=j, \\ 0, & \text{if } i\neq j. \end{cases} \tag{20}$$

$$\mathbf{B}_3 = \begin{bmatrix} \mathbf{0}_{n\times n} & -\mathbf{M}^{-1}\mathbf{B}^s_3 \\ \mathbf{0}_{n\times n} & \mathbf{0}_{n\times n} \end{bmatrix}, \tag{21}$$

where

$$B^s_{3ji} = \begin{cases} 0, & \text{if } i=j, \\ 0, & \text{if } i\neq j,\ i+j \text{ is even}, \\ 2ij/(j^2-i^2), & \text{if } i\neq j,\ i+j \text{ is odd}. \end{cases} \tag{22}$$

In Eq. (13), the axial transport velocity $v(t)$ is considered as a control input.

The vibration energy of the beam system can be represented as

$$E_{\text{beam}}(t) = \frac{1}{2}\int_0^l \{\rho[w_t(x,t)+v(t)w_x(x,t)]^2+Pw_x^2(x,t)+EIw_{xx}^2\}\mathrm{d}x, \tag{23}$$

where the first term on right side is the kinetic energy of the moving beam, the second term is caused by the beam tension, and the last term comes from the bending moment. Substituting Eq. (5) into Eq. (23) gives

$$E_{\text{beam}}(t) = \frac{1}{2}\int_0^l \left\{\rho\left[\sum_{i=1}^n(\dot q_i(t)\sin(i\pi x/l)+(i\pi v(t)/l)q_i(t)\cos(i\pi x/l))\right]^2 \right.$$
$$\left. +P\left[\sum_{i=1}^n(i\pi/l)q_i(t)\cos(i\pi x/l)\right]^2+EI\left[\sum_{i=1}^n(i\pi/l)^2q_i(t)\sin(i\pi x/l)\right]^2\right\}\mathrm{d}x. \tag{24}$$

The vibration energy (24) is then evaluated as

$$E_{\text{beam}}(t) \le \frac{1}{2}\int_0^l \left\{\rho\left[\sum_{i=1}^n(\dot q_i(t)+(i\pi v(t)/l)q_i(t))\right]^2+P\left[\sum_{i=1}^n(i\pi/l)q_i(t)\right]^2+EI\left[\sum_{i=1}^n(i\pi/l)^2q_i(t)\right]^2\right\}\mathrm{d}x$$

$$\leq \frac{l}{2}\left\{\rho\left[\sum_{i=1}^{2n}(1+\psi(i)(i\pi v(t)/l))s_i(t)\right]^2+P\left[\sum_{i=1}^{2n}(\psi(i)+(i\pi/l))s_i(t)\right]^2+EI\left[\sum_{i=1}^{n}(\psi(i)+(i\pi/l)^2)s_i(t)\right]^2\right\}, \tag{25}$$

where the Heaviside step function $\psi(i)$ is defined as

$$\psi(i)=\frac{1}{2}\{\mathrm{sgn}(i-n)+|\mathrm{sgn}(i-n)|\}. \tag{26}$$

From Eq. (25), the upper bound of the vibration energy (23) is obtained as

$$\overline{E}_{\mathrm{beam}}(t)=\frac{1}{2}\mathbf{s}^{\mathbf{T}}(t)\mathbf{Q}(t)\mathbf{s}(t), \tag{27}$$

where $\mathbf{Q}$ is a positive symmetric matrix of size $2n\times 2n$, and the elements of $\mathbf{Q}$ are defined as

$$Q_{ij}=\begin{cases} l\left\{\rho[1+i\pi v(t)\psi(i)/l]^2+P[\psi(i)+i\pi/l]^2+EI[\psi(i)+(i\pi/l)^2]^2\right\}, \text{if } i=j, \\ l\left\{\rho[1+i\pi v(t)\psi(i)/l][1+j\pi v(t)\psi(j)/l]+P[\psi(i)+i\pi/l][\psi(j)+j\pi/l]+EI[\psi(i)+(i\pi/l)^2][\psi(j)+(j\pi/l)^2]\right\}, \text{if } i\neq j. \end{cases} \tag{28}$$

Remark 3. It should be noted that if the upper bound of the vibration energy $\overline{E}_{\mathrm{beam}}(t)$ converges to zero, the vibration energy $E_{\mathrm{beam}}(t)$ also converges to zero. From Eq. (27), it is obvious that $\overline{E}_{\mathrm{beam}}(t)$ is represented in a linear quadratic form, which is a convenient form for application of the CG method. Therefore, the upper bound $\overline{E}_{\mathrm{beam}}(t)$ is used to establish the optimal control problem.

To solve the optimal control problem, the axial transport velocity $v(t)$ that minimizes the cost function is found as

$$J(t_f)=\frac{1}{2}\mathbf{s}^{\mathbf{T}}(t_f)\mathbf{Q}(t_f)\mathbf{s}(t_f), \tag{29}$$

where t_f is the terminal time, subjected to the state-space equations (13) with the initial and final conditions of the state vector

$$\mathbf{s}(0)=\mathbf{s}_0, \tag{30}$$

$$\mathbf{s}(t_f)=0, \tag{31}$$

and subjected to the inequality constraint of the control input

$$v(t)>0 \tag{32}$$

The initial state $\mathbf{s}(0)=\mathbf{s}_0$ can be obtained from the initial conditions (4). The constraint (31) can be combined with the cost function (29) as

$$\tilde{J}(t_f)=\frac{1}{2}\mathbf{s}^{\mathbf{T}}(t_f)\left[\mathbf{Q}(t_f)+\mathbf{W}\right]\mathbf{s}(t_f), \tag{33}$$

where $\mathbf{W}$ is a weight coefficient matrix of size $2n\times 2n$. In this paper, the function describing the axial transport velocity is assumed to be piecewise linear in every iteration of the CG algorithm. Therefore, from Eq. (13), the function $\mathbf{f}(\mathbf{s},v,\dot{v})$ can be represented as $\mathbf{f}(\mathbf{s},v)$. Note that, given an axial transport velocity $v(t)$, the state-space equations (13) can be solved for a unique $\mathbf{s}(v)$. Therefore, $\tilde{J}=\tilde{J}(v)$ is a unique function of $v(t)$. Let H denotes the Hamiltonian function given by

$$H(\mathbf{s},\boldsymbol{\lambda},v)=\boldsymbol{\lambda}^{\mathrm{T}}(t)\mathbf{f}(\mathbf{s},v), \tag{34}$$

where $\boldsymbol{\lambda}(t)$ is a $2n$-dimensional vector including adjoint variables. The necessary optimality conditions are then given as follows [37]:

$$\dot{\boldsymbol{\lambda}}(t)=-\frac{\partial H}{\partial \mathbf{s}}=-\mathbf{A}(t)\boldsymbol{\lambda}(t), \tag{35}$$

$$\boldsymbol{\lambda}(t_f)=[\mathbf{Q}(t_f)+\mathbf{W}]\mathbf{s}(t_f). \tag{36}$$

Then, the gradient is

$$g(t)=\frac{\partial H}{\partial v}=\boldsymbol{\lambda}^{\mathrm{T}}(t)\left[\mathbf{B}_1\mathbf{s}(t)+2v(t)\mathbf{B}_2\mathbf{s}(t)+b\mathbf{B}_3\mathbf{s}(t)\right]. \tag{37}$$

The CG direction of $v(t)$ in the kth iteration is determined as

$$p_k(t)=-g_k(t)+\beta_k p_{k-1}(t), \tag{38}$$

where

$$\beta_k = \frac{\int_0^{t_f} g_k(t) g_k(t) \mathrm{d}t}{\int_0^{t_f} g_{k-1}(t) g_{k-1}(t) \mathrm{d}t}, \tag{39}$$

and

$$g_k(t) = \left.\frac{\partial H}{\partial v}\right|_k. \tag{40}$$

Let $v_k(t)$ be the kth approximation to the proposed velocity profile. The new estimate of $v(t)$ is

$$v_{k+1}(t) = v_k(t) + \alpha_k p_k(t), \tag{41}$$

where α_k is chosen to minimize $\tilde{J}(v_k+\alpha_k p_k)$. The technique to search α_k is given in Ref. [40, Section 7]. The convergence of the CG algorithm is presented in Ref. [37].

Design procedure 1. The proposed control design using the CG algorithm to generate the proposed velocity profile is summarized as follows:

Step 1: Given t_f, $\mathbf{s}_0$, and v_0. Set $k=0$.

Step 2: Solve the state-space equations (13) forwards with $v=v_k$ and the adjoint Eqs. (35) and (36) backwards, and then compute p_k from Eq. (38). If $k=0$, then $p_0=-g_0$.

Step 3: Choose α_k to minimize $\tilde{J}(v_k+\alpha_k p_k)$. Set $v_{k+1}(t)=v_k(t)+\alpha_k p_k(t)$. If $v_{k+1}(t)<0$ then $v_{k+1}(t)=0$.

Step 4: Repeat steps 2 and 3 until

$$\left|\tilde{J}(v_{k+1}) - \tilde{J}(v_k)\right| < \delta \tilde{J}(v_k), \tag{42}$$

where δ is a specified positive number. If the condition (42) holds, then go to step 5.

Step 5: If $v=0$, stop; otherwise, set $\mathbf{s}_k \to \mathbf{s}_0$ and $v_k \to v_0$. Go to step 1.

Remark 4. Using Design procedure 1, which is based on the CG algorithm, it is guaranteed that the optimal value of the cost function $\tilde{J}^* = 0$ is achieved at the terminal time t_f. However, it is possible that the axial transport velocity reaches the zero value before the optimal value of the cost function is achieved. The strong technical advantage of the proposed control algorithm is that the vibration energy is assured to be suppressed completely within the deceleration time of the axial transport velocity, which can be selected by the designer.

Remark 5. In practice, a number of web materials such as films and textiles possess very small viscous damping coefficients, in which they can be assumed to be zero ($d_v=0$). This leads to the residual transverse vibration that cannot be suppressed without control. In this case, the proposed control method is well-suitable for the roll-to-roll systems, which are similar to the roll-to-roll lithography system presented in Section 1, where the conventional vibration, boundary, and distributed controls, are not able to be employed. This will be verified by numerical simulations in Section 4.

4. Simulations

To verify the effectiveness of the proposed control algorithm, numerical simulations were carried out with the system parameters listed in Table 1. The Galerkin method was applied to obtain the set of ODEs (6) with the number of functions of the approximate solution (5) $n=4$. Fig. 5 shows the two profiles for regulation of the axial transport velocity. In this simulation, the axial transport velocity decreased from the value of 2 m/s to zero with a deceleration time of 5 s. In the case of no vibration control, the conventional constant-deceleration velocity profile (dotted line), which has only a slope, was used. In this case, the moving web had a constant acceleration of 0.4 m/s^2 during the deceleration time. Meanwhile, the proposed velocity profile (solid line) generated using Design procedure 1 was constructed of 3 slopes. The optimal control problem was solved with the terminal time $t_f=5$, and the proposed profile of the axial transport velocity was obtained with 50 iterations of the CG algorithm. The weight coefficient matrix was chosen as $\mathbf{W}=\mathbf{I}$, where $\mathbf{I}$ is the identity matrix. Though the Galerkin method provides good predictions of the dynamic responses of axially moving systems, the Galerkin method should be carefully applied to axially moving beams translating with a high axial velocity [31], because the approximate solution (5) is constructed by employing eigenvalues of the stationary beam. Therefore, in this paper, the approximate dynamic model (10) was used only to design the proposed axial transport velocity profile. For numerical simulation purposes, the finite difference method was employed to find an approximate solution for the PDE (1) with the initial and boundary conditions given by Eqs. (2)–(4) and the time-varying velocity provided by the two profiles shown in Fig. 5. The convergence scheme is based on the central (for the beam span) and the forward/backward (for the left/right boundary) difference methods [45, Chapter 9].

Fig. 6 demonstrates the dynamic responses of the axially moving beam to two time-varying transport velocities (the proposed and conventional constant-deceleration profiles). As shown in Fig. 6(a), the vibration energy decays to zero in both cases. However, the convergence properties are different. In the control case (the proposed profile is used), the

Table 1
System parameter values used in numerical simulations.

Parameter	Description	Value
ρ	Mass per unit length	0.7 kg/m
I	Moment of inertia	0.34×10^{-6} m^4
E	Young's modulus	1.8×10^7 N/m^2
l	Distance between two rolls	4 m
d_v	Viscous damping coefficient	0.001 N m^{2}s
P	Tension	100 N
v_0	Initial axial velocity	5 m/s
$w_0(x)$	Initial transverse displacement	$0.05\sin(\pi x/l)$
$w_{t0}(x)$	Initial transverse velocity	0

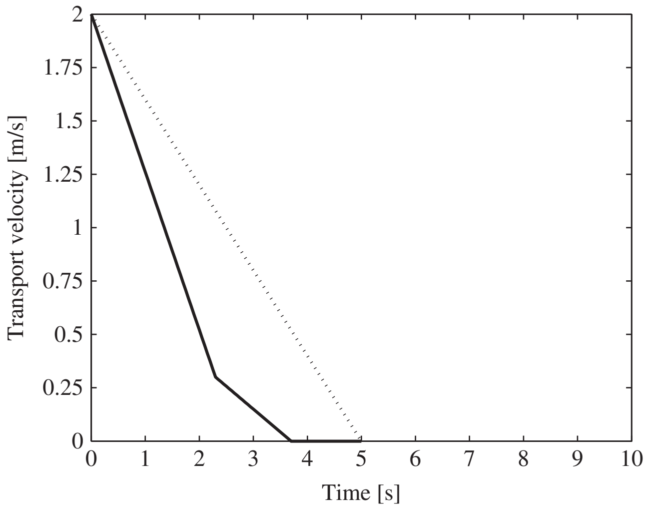

Fig. 5. Comparison of the proposed (solid line) deceleration profile and the conventional constant-deceleration (dotted line) profile in the presence of viscous damping $d_v=0.001$.

vibration energy (solid line) approaches the zero value at the time $t=5$; that is, the transverse vibration is suppressed completely within the deceleration time, as the control objective mentioned. This is consistent with the theoretical point inferred in Remark 4. In this case, when the axial transport velocity (solid line) reaches zero at the time $t=3.7$, $E_{\text{beam}}(3.7)=16$. After the axial transport velocity reaches zero, the residual vibration energy converges slowly to zero within 1.3 s. From the physical point of view, as mentioned in Section 3, plenty of time is required if the transverse vibration is suppressed by only the viscous damping force. Therefore, the residual vibration energy should approach a small value when the axial transport velocity reaches zero. In this paper, this control strategy was executed using the CG method. The theoretical basis of the application of the CG method is that the vibration energy decays most quickly between two consecutive iterations of the CG algorithm. As shown in Fig. 6(a), this theoretical point was verified. In the case of control, comparing $E_{\text{beam}}(0)=2500$ and $E_{\text{beam}}(3.7)=16$, it can be concluded that the vibration energy is almost suppressed when the axial transport velocity reaches zero. In the case of no control, it seems that the convergence speed of the vibration energy (dotted line) does not change during the deceleration time. According to conventional constant-deceleration profile, suppression of the vibration energy takes 9 s. Moreover, when the axial transport velocity reaches zero at $t=5$, the value of the residual vibration energy is considerable ($E_{\text{beam}}(5)=66$). It was shown that the vibration energy in the case of no vibration control decays more slowly than in the case of vibration control, especially when the axial transport velocity decreases from the initial value to zero. The convergences of the transverse displacements of the axially moving beam at $x=l/2$ to zero in the two cases (with control and without control) were compared, as shown in Fig. 6(b).

In the case of the viscous damping coefficient that was assumed to be zero ($d_v=0$), the axial velocity profile for vibration suppression (solid line) was proposed as shown in Fig. 7. The system parameters (except the viscous damping coefficient) were maintained as in the case of the viscous damping coefficient that was involved. The simulation results shown in Fig. 8(a) and (b) indicate that when the conventional constant-deceleration profiles are used, the vibration energy (dotted-line) cannot converge to zero without the presence of the viscous damping force. Meanwhile, the transverse vibration is still suppressed completely by regulation of the axial transport velocity as the proposed profile. Through a comparison of the simulation results (time of vibration suppression and control performance) for control and no

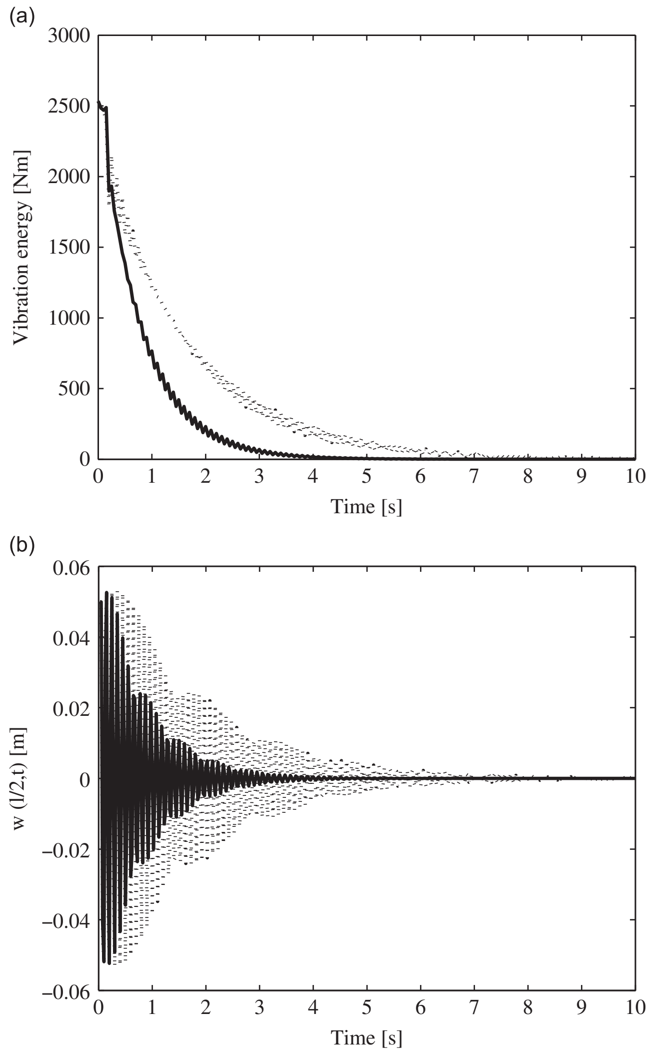

Fig. 6. Comparison of the vibration energies and the transverse displacements in the presence of viscous damping $d_v=0.001$ (controlled-solid line vs. uncontrolled-dotted line): (a) convergence of the vibration energies and (b) convergence of the transverse displacements at $x=l/2$.

control, the considerable improvement effected by applying the control algorithm to the beam system for vibration suppression was verified.

In practice, since the exact value of the viscous damping may not be obtainable, Fig. 9 is provided to illustrate the effect of the modeling error in the viscous damping to the residual vibration energy. The velocity profile shown in Fig. 5 (designed for the case of $d_{v,\text{model}}=0.001$) is applied to the beam systems under the actual viscous damping $d_{v,\text{actual}}= d_{v,\text{model}} \pm \Delta d_v$, where $0 \le \Delta d_v \le 0.001$. The residual vibration energies at $t_f=5$ are plotted vs. the ratios $d_{v,\text{actual}}/d_{v,\text{model}}$. As shown in Fig. 9, the effect of the viscous damping modeling error in the case of $d_{v,\text{actual}} > d_{v,\text{model}}$ is lower than the one in the case of $d_{v,\text{actual}} < d_{v,\text{model}}$.

5. Conclusions

In this paper, a control algorithm that uses the effects of the time-varying axial transport velocity to suppress the transverse vibration of an axially moving beam was developed. The basis of the proposed control algorithm is the regulation of the axial transport velocity to track the proposed profile according to which the vibration energy decays most quickly. With regard to the dynamics of the axially moving beam, the Galerkin method was applied to reduce the PDE into a set of ODEs, which was rewritten into state-space equations. A design procedure based on the CG method was introduced to generate the proposed velocity profile. Compared with the case of no control, the proposed control algorithm provided considerably improved suppression of the vibration energy. It is believed that the proposed control algorithm is the first solution using the regulation of the axial transport velocity to suppress the transverse vibration. This also provides a viable

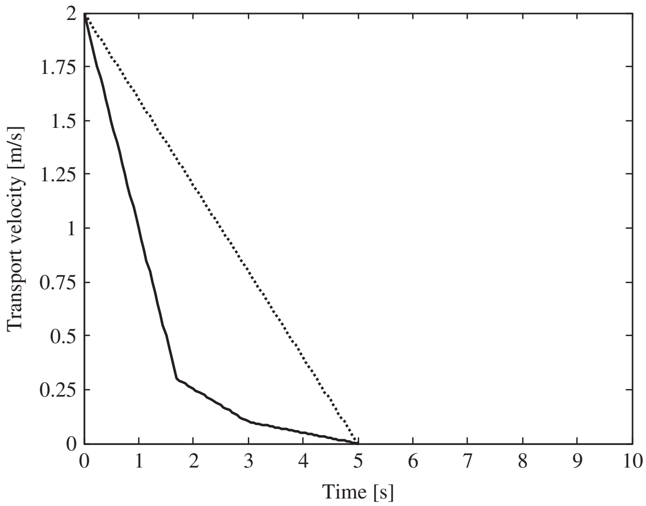

Fig. 7. Deceleration profile generated from the proposed method (solid line) when the viscous damping does not exist.

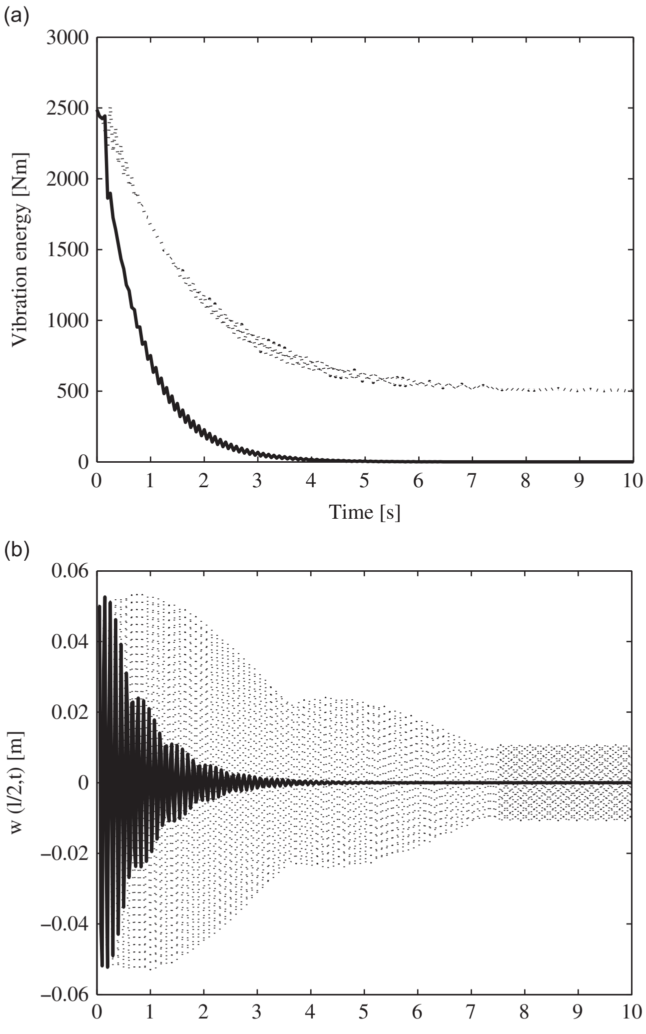

Fig. 8. Comparison of the vibration energies and the transverse displacements in the case of no viscous damping (controlled-solid line vs. uncontrolled-dotted line): (a) convergence of the vibration energies and (b) convergence of the transverse displacements at $x = l/2$.

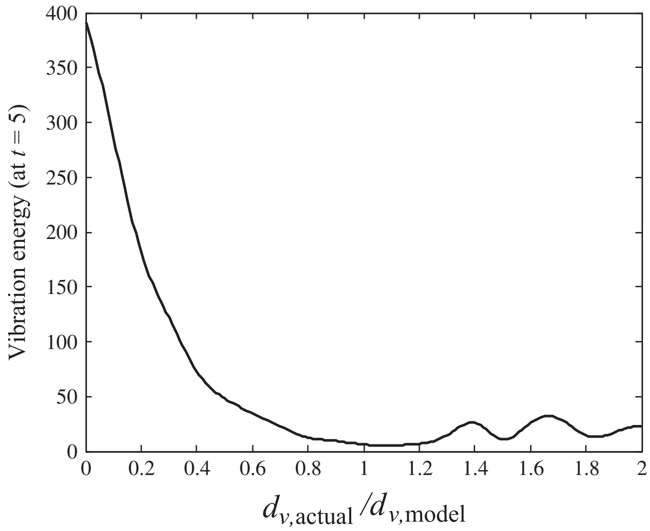

Fig. 9. Effect of the modeling error in the viscous damping to the residual vibration energy.

solution to the problem of the vibration control of axially moving systems when the application of boundary control technique is impossible.

Acknowledgment

This work was supported by the Regional Research Universities Program (Research Center for Logistics Information Technology, LIT) and the World Class University (grant no. R31-20004) granted by the National Research Foundation of Korea under the Ministry of Education, Science and Technology, Korea.

References

[1] K. Jain, M. Klosner, M. Zemel, Flexible electronics and displays: high-resolution, roll-to-roll, projection lithography and photoablation processing technologies for high-throughput production, *Proceedings of the IEEE* 93 (8) (2005) 1500–1510.
[2] M. Pakdemirli, A.G. Ulsoy, A. Ceranoglu, Transverse vibration of an axially moving accelerating string, *Journal of Sound and Vibration* 169 (2) (1994) 179–196.
[3] A.E. Jain, A.J. Pritchard, Sensors and actuators in distributed systems, *International Journal of Control* 46 (4) (1987) 1139–1153.
[4] R.-F. Fung, J.W. Wu, S.L. Wu, Exponential stabilization of an axially moving string by linear boundary feedback, *Automatica* 35 (1) (1999) 177–181.
[5] Z. Qu, Robust and adaptive boundary control of a stretched string on a moving transporter, *IEEE Transactions on Automatic Control* 46 (3) (2001) 1045–1054.
[6] R.-F. Fung, J.W. Wu, P.Y. Lu, Adaptive boundary control of an axially moving string system, *Journal of Vibration and Acoustics—Transactions of the ASME* 124 (3) (2002) 435–440.
[7] S.P. Nagarkatti, F. Zhang, B.T. Costic, D.M. Dawson, Speed tracking and transverse vibration control of axially moving accelerating web, *Mechanical Systems and Signal Processing* 16 (2-3) (2002) 337–356.
[8] M.S. de Queiroz, C.D. Rahn, Boundary control of vibration and noise in distributed parameter systems: an overview, *Mechanical Systems and Signal Processing* 16 (1) (2002) 19–38.
[9] P.C.-P. Chao, C.-L. Lai, Boundary control of an axially moving string via fuzzy sliding-mode control and fuzzy neural network methods, *Journal of Sound and Vibration* 262 (4) (2003) 795–813.
[10] K.-J. Yang, K.-S. Hong, F. Matsuno, Robust adaptive boundary control of an axially moving string under a spatiotemporally varying tension, *Journal of Sound and Vibration* 273 (4-5) (2004) 1007–1029.
[11] K.-J. Yang, K.-S. Hong, F. Matsuno, Robust boundary control of an axially moving string using a PR transfer function, *IEEE Transactions on Automatic Control* 50 (12) (2005) 2053–2058.
[12] T.-C. Li, Z.-C. Hou, J.-F. Li, Stabilization analysis of a generalized nonlinear axially moving string by boundary velocity feedback, *Automatica* 44 (2) (2008) 498–503.
[13] Q.C. Nguyen, K.-S. Hong, Asymptotic stabilization of a nonlinear axially moving string by adaptive boundary control, *Journal of Sound and Vibration* 329 (22) (2010) 4588–4603.
[14] Y. Li, C.D. Rahn, Adaptive vibration isolation for axially moving beams, *IEEE/ASME Transactions on Mechatronics* 5 (4) (2000) 419–428.
[15] W.D. Zhu, J. Ni, Energetics and stability of translating media with an arbitrary varying length, *Journal of Vibration and Acoustics—Transactions of the ASME* 122 (3) (2000) 295–304.
[16] R.-F. Fung, J.-H. Chou, Y.-L. Kuo, Optimal boundary control of an axially moving material system, *Journal of Dynamic Systems, Measurement, and Control—Transactions of the ASME* 124 (1) (2002) 55–61.
[17] K.-J. Yang, K.-S. Hong, F. Matsuno, Energy-based control of axially translating beams: varying tension, varying speed, and disturbance adaptation, *IEEE Transactions on Control Systems Technology* 13 (6) (2005) 1045–1054.
[18] B.V.E. How, S.S. Ge, Y.S. Cho, Active control of flexible marine risers, *Journal of Sound and Vibration* 320 (4-5) (2009) 758–776.
[19] S.S. Ge, W. He, B.V.E. How, Y.S. Choo, Boundary control of a coupled nonlinear flexible marine riser, *IEEE Transactions on Control Systems Technology* 18 (5) (2010) 1080–1091.

[20] M. Stylianou, B. Tabarrok, Finite element analysis of an axially moving beam, Part II: stability analysis, *Journal of Sound and Vibration* 178 (4) (1994) 455–481.
[21] G. Chakraborty, A.K. Mallik, Stability of an accelerating beam, *Journal of Sound and Vibration* 227 (2) (1999) 309–320.
[22] H. Okubo, K. Tanako, O. Matsushita, K. Watanabe, Y. Hirase, Vibration and control of axially moving belt system: analysis and experiment and parametric excitation, *Journal of Vibration and Control* 6 (4) (2000) 589–605.
[23] H.R. Oz, M. Pakdemirli, H. Boyacı, Non-linear vibrations and stability of an axially moving beam with time-dependent velocity, *International Journal of Non-Linear Mechanics* 36 (1) (2001) 107–115.
[24] R.G. Parker, Y. Lin, Parametric instability of axially moving media subjected to multifrequency tension and speed fluctuation, *Journal of Applied Mechanics—Transactions of the ASME* 68 (1) (2001) 49–57.
[25] K.-Y. Lee, A.A. Renshaw, A numerical comparison of alternative Galerkin methods for eigenvalues estimation, *Journal Sound and Vibration* 253 (2) (2002) 359–372.
[26] F. Pellicano, F. Vestroni, Complex dynamics of high-speed axially moving systems, *Journal of Sound and Vibration* 258 (1) (2002) 31–44.
[27] K. Marynowski, T. Kapitaniak, Kelvin–Voigt versus Burgers internal damping in modeling of axially moving viscoelastic web, *International Journal of Non-Linear Mechanics* 37 (7) (2002) 1147–1161.
[28] G. Suweken, W.T. Van Horssen, On the transversal vibrations of a conveyor belt with a low and time-varying velocity. Part II: the beam-like case, *Journal of Sound and Vibration* 267 (5) (2003) 1007–1027.
[29] F. Pellicano, G. Catellani, A. Fregolent, Parametric instability of belts: theory and experiments, *Computers and Structures* 82 (1) (2004) 81–91.
[30] K. Liu, L. Den, Identification of pseudo-natural frequencies of an axially moving cantilever beam using a subspace-based algorithm, *Mechanical Systems and Signal Processing* 20 (1) (2006) 94–113.
[31] G. Cepon, M. Boltezar, Computing the dynamic response of an axially moving continuum, *Journal of Sound and Vibration* 300 (1-2) (2007) 316–329.
[32] S.V. Ponomareva, W.T. van Horssen, On transversal vibration of an axially moving string with a time-varying velocity, *Nonlinear Dynamics* 37 (1–2) (2007) 315–323.
[33] T.G. Hayes IV, B. Bhushan, Vibration analysis of axially moving magnetic tape with comparison to static and dynamic experiment results, *Microsystem Technologies* 13 (7) (2007) 689–699.
[34] H. Ding, L.-Q. Chen, Galerkin methods for natural frequencies of high-speed axially moving beams, *Journal of Sound and Vibration* 329 (17) (2010) 3484–3494.
[35] M.R. Kermani, Analytic modal analyses of a partially strengthened Timoshenko beam, *IEEE Transactions Control Systems Technology* 18 (4) (2010) 850–858.
[36] L.H. Chen, W. Zhang, F.H. Yang, Nonlinear dynamics of higher-dimensional system for an axially accelerating viscoelastic beam with in-plane and out-plane vibrations, *Journal of Sound and Vibration* 329 (25) (2010) 5321–5345.
[37] L.S. Lasdon, S.K. Mitter, A.D. Waren, The conjugate gradient method for optimal control problems, *IEEE Transactions on Automatic Control AC* 12 (2) (1967) 132–138.
[38] S.S. Tripathi, K.S. Narendra, Optimization using conjugate gradient methods, *IEEE Transactions on Automatic Control AC* 15 (2) (1970) 268–270.
[39] D.P. Berteskas, Partial conjugate gradient methods for a class of optimal control problems, *IEEE Transactions on Automatic Control AC* 19 (3) (1974) 209–217.
[40] J.C. Heideman, A.V. Levy, Sequential conjugate-gradient-restoration algorithm for opitimal control problems. Part1. Theory, *Journal of Optimization Theory and Applications* 15 (2) (1975) 203–222.
[41] E.R. Edge, W.F. Power, Function-space quasi-Newton algorithms for optimal control problems with bounded controls and singular arcs, *Journal of Optimization Theory and Applications* 20 (4) (1976) 455–479.
[42] M. Bocek, Conjugate gradient algorithm for optimal control problems with parameters, *Kypernetika* 16 (5) (1980) 454–461.
[43] F.-S. Wang, C.-T. Su, Y.-C. Liu, Computation of optimal feedforward and feedback control by a modified reduced gradient method, *Applied Mathematics and Computation* 104 (1) (1999) 85–100.
[44] J. Kasac, J. Deur, B. Novakovic, I.V. Kolmanovsky, A conjugate gradient-based BPTT-like optimal control algorithm, in: *Proceedings of the 18th IEEE International Conference Control Applications*, Saint Petersburg, Russia, 2009, pp. 861–866.
[45] W.Y. Yang, W. Cao, T.S. Chung, J. Morris, *Applied numerical methods using Matlab*, John Willey & Sons, New Jersey, USA, 2005.